

Soft Matter

Accepted Manuscript



This is an *Accepted Manuscript*, which has been through the Royal Society of Chemistry peer review process and has been accepted for publication.

Accepted Manuscripts are published online shortly after acceptance, before technical editing, formatting and proof reading. Using this free service, authors can make their results available to the community, in citable form, before we publish the edited article. We will replace this *Accepted Manuscript* with the edited and formatted *Advance Article* as soon as it is available.

You can find more information about *Accepted Manuscripts* in the [Information for Authors](#).

Please note that technical editing may introduce minor changes to the text and/or graphics, which may alter content. The journal's standard [Terms & Conditions](#) and the [Ethical guidelines](#) still apply. In no event shall the Royal Society of Chemistry be held responsible for any errors or omissions in this *Accepted Manuscript* or any consequences arising from the use of any information it contains.



Journal Name

ARTICLE

Co-assembly of Polyoxometalates and Peptides towards Biological Applications

Peng-Fan Gao, Yuqing Wu* and Lixin Wu*

Received 00th January 20xx,
Accepted 00th January 20xx

DOI: 10.1039/x0xx00000x

www.rsc.org/

The synergistic self-assembly of biomolecules with polyoxometalates (POMs) has recently been considered as an effective approach to construct nano-biomaterials with diverse structures and morphologies towards the applications in drug delivery, controlled release, tissue engineering scaffold, and biomineralization, due to the unique features of the clusters in addition to many well-known inorganic nanoparticles. This review presents an overview of recent works focusing on the noncovalent co-assembly of peptides and POMs as well as their biological applications. In the co-assemblies triggered by the interaction between components significant advantages that POMs or peptides alone do not possess come out accompanied by chiral recognition of hybrid metal oxides, the quickly hydrolysis of peptide, and the enhanced inhibition of A β aggregation and so forth. Finally, we outline a brief perspective on possible unresolved issues and future opportunities in this field.

Introduction

Self-assembly, a common process at all scales, are emerging as a powerful, bottom-up approach for the fabrication of novel functional nano-or bio-materials.^{1,2} Being characterized by spontaneous diffusion and specific association of molecules self-assembly dictated by non-covalent interactions as hydrogen bonds, electrostatic interaction, π - π stacking, hydrophobic forces, non-specific van der Waals forces, and chiral dipole-dipole interactions.^{3,4} It has proven that numerous molecular entities, such as organic compounds, proteins, peptides, DNA and others can be used to construct the bio-functional materials.⁵ Among them peptides are one of the most promising ones as they have the intrinsic ability to self-assemble into versatile biological architectures.⁶ For example, a dipeptide of L-Phe-L-Phe (FF) could assemble to nanotubes with a long persistence length (\sim 100 nm) by a combination of hydrogen bonding and π - π stacking of aromatic residues⁷ and then transitioning to vesicle-like structures at higher concentrations (\geq 100 mg/ml) by dissolving the lyophilized peptide in 1,1,1,3,3,3 hexafluoro-2-propanol;⁷ they can also form nanofibrils and ribbons with the protection of 9-fluorenylmethoxycarbonyl (Fmoc) in water and thus results in a hydrogel being held together in a network by hydrogen bonding and π - π interaction.⁸ In addition, Han *et al.* reported the NH₂-Phe-Phe-COOH di-peptide could be capable self-

assemble into individually-dispersed and rigid nanowires.⁹ The self-assembly of peptides have presented lots of superiority such as highly chemical/thermal stability,^{10,11} chemical diversity¹² and mechanical strength.¹³ And they are much more robust and can be readily synthesized on a large scale.¹² However, additional properties are critically required for optical, electrical, or others purposes for such nano-biomaterials, which would be more suitable for potential applications in nanomaterials.

Polyoxometalates (POMs) are a diverse family of metal oxide clusters, with defined architectures and variable, especially controlled sizes in the nanometre range.¹⁴ Among different areas of inorganic chemistry metal oxide-based POM clusters represent a class of materials that exhibiting matched structural versatility and unique intrinsic properties.¹⁵⁻¹⁹ This determined the POMs can be applied to optical, catalyst, medicine science and so on. For a long term, POM clusters were tried to be used in antitumor and antibacterial as well as other bioactivities due to the properties differing from general small molecules. However, the possible toxicity and instability of POMs as drugs restrict the *in vivo* applications. In contrast, the outstanding structural and morphologic properties make them excellent candidates for the promotion of self-assembly of peptides and other biomolecules. As a sign, the investigations on the combination of POMs with peptides and proteins are of much interest in the past several years.

In optics, most of POMs are weakly or even not luminescent. However, as the luminescence of rare-earth metal ions is known to be sensitive to the environment, the incorporation of them into POMs has put some unique optical property for the materials. Several special rare-earth atoms have been

State Key Laboratory of Supramolecular Structure and Materials, Jilin University, No. 2699 Qianjin Street, Changchun 130012, China E-mail: yqw@jlu.edu.cn; wulx@jlu.edu.cn.

added in POMs with different structural morphologies.^{20,21} Among them, europium-containing POMs have shown strong and sensitive luminescent effects which have been used in diversity aspects.^{22,23} For example, Hungerford *et al.* studied the interaction of a series of europium containing POMs with serum albumin (SA) making use of the luminescence enhancement and discovered the types of POMs were very important in the interaction.^{24,25} Zhang *et al.* achieved a facile fabrication of core-shell nanostructures using a photoluminescent Eu-containing POM with double hydrophilic neutral-cationic block copolymer, poly(ethyleneoxide-*b*-N,N-dimethylaminoethyl methacrylate) (PEO₁₁₄-*b*-PDMAEMA₁₆), in aqueous solution. Through electrostatic interaction the emission of Eu-POM was enhanced as much as 20 times *via* complexation with the cationic block, N,N-dimethylamino ethylmethacrylate (PDMAEMA).²⁶ Li *et al.* found the K₁₃[Eu(SiW₁₀MoO₃₉)₂·28H₂O] could be used as a suitable luminescence probe which demonstrated the selective interaction with basic amino acids(AAs).²⁷ Recently, we reported a two-step binding process of Eu-Containing POMs, K₁₃[Eu(SiW₉Mo₂O₃₆)₂·28H₂O (EuSiW_{Mo}), to BSA basing on the change of luminescence enhancements and revealed the intrinsic mechanism of the complicated interaction.²⁸ In regarding the luminescence property of POMs which have been demonstrated in many studies, the versatile bio-applications, especially the typical ones should be mentioned. In addition, in the aspects of self-assembly, there are a kind of unique POMs with a rigid framework, mono-dispersed size, water solubility, and biofunctionality.²⁹⁻³² They can assemble with several of functional materials and then be extensively enlarged of their applications. For example, in morphologies, some of them can self-assemble into “blackberry” structure,³³ while others to form two-dimensional films, one-dimensional fibres, tubes or belts, zero-dimensional capsules,³⁴ and vesicles, through different fabrication ways such as self-assembled monolayers (SAMs), layer-by-layer (LbL) and Langmuir-Blodgett (LB) films. Some of them can assemble with organic like PEGylation,³⁵ while others can assemble with biomolecular like folate,³⁶ DNA,³⁷ enzymes,³⁸ peptides^{39,40} and formed the spherical particles and so on. In medical science, as important inorganic drug candidates, POMs have shown promising antiviral and antitumor activities for more than decades.⁴¹ The last twenty years has witnessed a growing interest in the biological properties of POMs and their applications in medicine.⁴² Deborah *et al.* addressed Nb-containing POMs of the Wells-Dawson class, K₇H[Nb₆O₁₉], inhibit HIV-1 protease (HIV-1P) by a new mode based on the detailed kinetics, binding, and molecular modelling studies.⁴³ Qu’s group found that POMs could be the inhibitors to prevent Aβ aggregation, and the size of POMs played a key role in Aβ recognition and amyloid inhibition.⁴¹ However, the driving force in the interactions between POMs and Aβ is essential electrostatic effect, a non-specific interaction. It has been reported that non-specific targeting also occurs in larger Aβ assemblies and may cause oligomer-derived toxicity.⁴⁴ Further studies also concerning the cellular uptake of antiviral POMs and the lower biocompatible.⁴⁵ Therefore, in order to find

more suitable inhibits or functionalized POMs and to find the biological mechanism and theories further, more and more researchers started to investigate the self-assembly of POMs and peptides, which will be summarized in section 3.

A lot of achievements at molecular level for protein-POMs interactions have been gained, in which several factors such as the size, shape and nature of the embedded metal ion in the architecture of POM are demonstrated to be crucial in governing the interactions.^{24,25,32,46} Zhang *et al.* reported the interaction between human serum albumin (HSA) and a Keggin-type POM, [H₂W₁₂O₄₀]⁶⁻ (H₂W₁₂) as well as a wheel-shaped [NaP₅W₃₀O₁₁₀]¹⁴⁻ (P₅W₃₀), where the binding was mainly attributed to the electrostatic interaction.⁴⁷⁻⁴⁹ Zheng *et al.* studied the interaction of europium decatungstate [EuW₁₀O₃₆]⁹⁻ and histone H1, which supplied the binding constants and the change of the protein secondary structure.⁵⁰ In addition, Goovaerts *et al.* calculated the association constants of several Keggin-type POMs with BSA and HSA, and pointed out the binding site at the surface of albumins.⁵¹ They also studied the regioselective hydrolysis of HSA by Zr(IV)-substituted polyoxotungstates using tryptophan fluorescence spectroscopy.⁵² Though the progress has greatly enriched the knowledge on the interactions between POMs and proteins, the binding mechanism and the possible intrinsic factors, particularly the binding sites, binding kinetics and especially the driving force in association with the basic properties of POMs and proteins, were still far from clarification. Therefore, it is necessary to study the interactions between POMs and the specific peptides from proteins.

The biological application of POMs and peptides assemblies has attracted more and more attention because of the unique superiorities, such as better biocompatible and control optical properties than POMs; higher water solubility and easily detection than peptides itself. And also, the self-assembly combined the advantages both of peptides and POMs, which promoted a way in biochemistry such as drugs delivery. So the study of self-assembly of POMs and peptides was very important and indispensable in biology, which has been proved in the inhibition of AD disease.

Though this field is growing at an accelerating pace, there exist no reports to comprehensively summarize the development and the application of POMs-peptides (be defined as POMs@P) building blocks for molecular self-assembly. Therefore, in this review, we will summarize the self-assembly of POMs-peptides and the bio-applications of them. We will also discuss the potential applications of such assembled functional materials in drug delivery, biosensors, guest encapsulation and so on.

2. Co-assembly of POMs and amino acids

Amino acids, as the basic units of proteins, have won much attention in combination with POMs owing to their potential antiviral activities. Xin *et al.* reported the syntheses and structural characterization of Tin(II) tungstophosphate as well as the tungstosilicate derivatives [Sn(II)₃(α-PW₉O₃₄)₂]¹²⁻ (**1**), [Sn(II)₃(α-SiW₉O₃₄)₂]¹⁴⁻ (**2**), and [Sn(II)₃(β-SiW₉O₃₄)₂]¹⁴⁻ (**3**), which were prepared by reaction of tin(II) sulfate with Na₈H[α,

β -PW₉O₃₄·24H₂O, Na₁₀[β -SiW₉O₃₄] \cdot xH₂O, and Na₁₀[α -SiW₉O₃₄] \cdot 26H₂O, respectively.⁵³ All three anions display one-line ¹¹⁹Sn-NMR and two-line ¹⁸³W-NMR (intensity 1:2) spectra. However, when lysine-HCl was added to the solution containing **1**, the ³¹P and ¹¹⁹Sn-NMR spectra were unchanged; but the ¹⁸³W-NMR spectrum showed three lines, while there had no significant effect on the broad Sn- and W-NMR lines as for **2** and **3**. In addition, the W-NMR spectra were collected on samples containing **1** and lysine-HCl with molar ratios ranging from 1:1 to 1:20 in order to study the influence of lysine concentration on the belt-tungsten W-NMR line splitting. The data plotted were consistent with the formation of a labile complex of **1** with lysine, which was similar with other amino acids as isoleucine, and histidine. An attempt was made to isolate crystals of the lysine complex of **1**, but which could not be solved owing to the considerable disorder and no firm conclusion can be reached in the absence of a structure of an amino acid complex.

After that, Liu *et al.* offered the first structure information about the amino acid–polyoxometalate complex.⁵⁴ The crystal structure of (Lys)₂H₆[P₂-Mo₁₈O₆₂] \cdot 16H₂O was consisted by [P₂Mo₁₈O₆₂]⁶⁻ unit and lysine with a ratio 1:2. The crystallographical data and the bond distances analysis indicated the independent atoms with atomic numbers in the crystal structure were displaced in Fig. 1, where the water and lysine interacted with the 18-molybdodiphosphoric anion *via* hydrogen bonding. They also studied the (Lys)₂H₆[P₂-Mo₁₈O₆₂] \cdot 16H₂O by IR spectra and ³¹P NMR spectrum and found the IR bands arising from the polyoxoanion changed obviously either in intensities or in positions comparing the precursors 18-molybdodiphosphoric acid. The study provided information on the model interaction between the POMs and AAs, which paved a way further to explore the interaction of POMs and protein.

In 2006, Wang *et al.* reported nanotubes constructed from amino acid and POM as a type of versatile organic–inorganic hybrid material by using tyrosine (Tyr) and the corresponding Keggin-type heteropoly acids, H₃PMo₁₂O₄₀·13H₂O, H₃PW₁₂O₄₀·3H₂O and H₄SiW₁₂O₄₀·5H₂O, respectively.⁵⁵ Such nanotubes was synthesized by one-step solid-state chemical reaction at room temperature and finally formed (HTyr)₃PMo₁₂O₄₀·3H₂O, (HTyr)₃PW₁₂O₄₀·3H₂O, and

(HTyr)₄SiW₁₂O₄₀·5H₂O, respectively, in a convenient and rapid synthesis way. The IR spectra of the as-synthesized samples and the reactants indicated the Tyr was protonated and the Tyr cation (HTyr⁺) was generated when reacted with the heteropoly acids. The NMR analysis and XRD patterns combined with IR spectra indicated the samples possessed Keggin-type structures. They also provided the morphology of the product by SEM and TEM and displayed the nanotubes have diameters from 50 to 150 nm and lengths up to several micrometres. They also discovered that the product was obviously different if the Tyr was replaced by phenylalanine (Phe), which formed nanoparticles.⁵⁶ The differences observed between them were suggested to be due to the structures of Tyr (HO–Ph–CH₂–CH(NH₂)COOH) and Phe (Ph–CH₂–CH(NH₂)COOH), where Tyr has a hydroxyl group on the benzene ring while the Phe has not. Then they confirmed the hypothesis by using other amino acids, such as an aromatic-series amino acid—Phenylalanine (Phe), a fatty-series amino acid—threonine (Thr), and a heterocycle-series amino acid—tryptophane (Trp), *via* a one-step solid-state chemical reaction with heteropoly acids at room temperature. However, the detailed mechanism behind the Tyr-POM tubular structure was not under investigated in this study.

After that, Kong *et al.* studied the interaction of AAs and POMs at other point.⁵⁷ They first reported the assembly of AA-H₃[PMo₁₂O₄₀] \cdot nH₂O (PMO₁₂) in nanorods with an average diameter of 50–80 nm forming through reverse micelles under a solvent-thermal condition by using H₃[PMo₁₂O₄₀] \cdot xH₂O and amino acids as glycin (Gly), lysine (Lys) and histidine (His). In following, the inhibitory activity for the nanorod-AA-PMO₁₂ samples against *E. coli* was assessed. The antibacterial test indicated the nanorod-Gly-PMO₁₂ exhibited significant antibacterial activity compared to the bulky crystal (Gly)₃[PMo₁₂O₄₀] and submicrometer rods-Gly-PMO₁₂ (SMR-Gly-PMO₁₂), which demonstrated well the importance of nanosize effect. This result provided a feasible example of actual use of the nanorod-AA-POM materials and illustrated the vital of the self-assembly of POMs and amino acids.

Recently, Li *et al.* studied the selective interaction between the AAs and POMs and demonstrated the intrinsic binding mechanism.²⁷ They selected europium-substituted POMs, K₁₃[Eu(SiW₁₀MoO₃₉)₂] \cdot 28H₂O (EuSiWMo), K₁₁[Eu(PW₁₁O₃₉)₂] (EuPW11) and K₉[EuW₁₀O₃₆](EuW10) with different negatively charged AAs to investigate the interactions of POMs with most

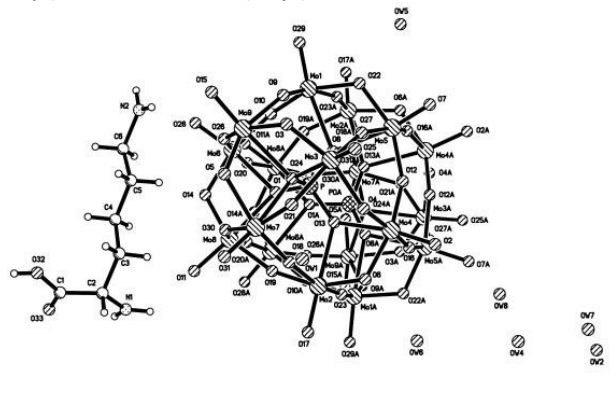


Fig. 1 Molecular structure of C₁₂H₆₆Mo₁₈N₄O₈₂P₂ with hydrogen bonds represented by dashed lines.⁵⁴

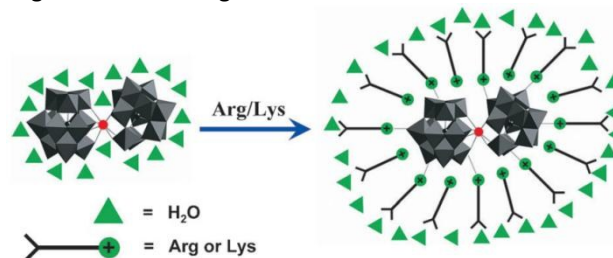


Fig. 2 Model of the interaction between basic AAs and EuSiWMo. Representative structures of basic AAs, anionic POM EuSiWMo, and the aggregated nanostructures of their complex in water.²⁷

AAs in aqueous solutions (Fig. 2). Finally, the most promising results were obtained by using the environmental sensitive EuSiWMo. The largely enhanced emissions of the Eu(III) were observed in the presence of 1.0 mM basic AAs as L-Lys, L-Arg, and L-His; while there was no clear change observed for others AAs. The UV/Vis absorption and CD spectrum confirmed the microenvironment of the Eu(III) center did not change much upon binding with the basic AAs. Then they explored the intrinsic mechanism of the AA-induced luminescence enhancement of Eu(III) by the following several techniques. The isoelectric points of the AAs were firstly analysed which suggested the positively charged residues of the basic AAs were the dominant binding sites for the recognition. Then, the ^1H NMR experiments were performed in D_2O to explore the detailed binding sites. The chemical shift of $\text{H}(\alpha-\epsilon)$ in L-Lys all showed up-field shifts upon the addition of EuSiWMo, indicating the electron-donating nature of EuSiWMo to the amino group after binding. The larger chemical shift of the $\text{H}(\epsilon)$ and $\text{H}(\gamma)$ protons in L-Lys suggested that the binding site was located at the amino group of L-Lys residual. The slight chemical shift of $\text{H}(\alpha)$ linked to the chiral carbon atom excluded the possibility of binding to another amino group near to it, which were further proved by the similar binding results of L-Arg/L-His to EuSiWMo. In combining with the results from non-basic AAs, they concluded the binding sites between EuSiWMo and basic AAs were located at the residual guanidine for L-Arg and the imidazole group for L-His, which were identical to interactions between EuSiWMo and L-Lys at the amino group in residual. The larger chemical shifts of protons in the basic residue of AAs illustrated they were the vital binding sites for the selective recognition of EuSiWMo. When using another two POMs, $\text{K}_{11}[\text{Eu}(\text{PW}_{11}\text{O}_{39})_2]$ and $\text{K}_9[\text{EuW}_{10}\text{O}_{36}]$, they found the basic AAs could not induce much increase in the Eu(III) emission, which demonstrated the amount of negative charges at the POM surface was vital for its selective binding to basic AAs. In following, the fluorescence lifetime differences for EuSiWMo in the absence and presence of AA confirmed it was indeed closely bound to the basic AAs; while the non-interaction between the ester derivatives of Lys, Arg, and Leu and EuSiWMo emphasized the strong electrostatic interactions occurring between POMs and AAs. Comparing to another report which studied the interaction of POMs and a dipeptide Gly-Gly,⁵⁸ they found similar chemical structures between POMs and AAs. That was, the amino group in basic AA was functionalized as a proton donor for the hydrogen bond formation, being a big assistance to the dominant electrostatic contribution when the AA interacted with the POM. Therefore, this study not only provided an example of the assembly of POMs and AAs, but it also illustrated additionally the mechanism of the interaction was attributed to the electrostatic interactions and hydrogen bonds. Such report was meaningful to further understand the interactions, especially the binding sites between POMs and peptides, or proteins.

3. Co-assembly of peptides and POMs

An understanding of the conditions and methods are critical for the study of these co-assembly process. For example, the type of POMs and the feature of peptides, the mode of the action and the characteristic of nanoparticles are all vital in the co-assembly. In this section, we will describe the various methods, especially the good examples, developed over the past decade by a time sequence, and also introduce the potential superiorities of the assemblies at the same time.

3.1 Co-assembly of vanadium-containing POMs and dipeptide

The existence of vanadium-requiring enzymes and the potent biological activities of vanadium in biological systems have gained increasing interest in the coordination chemistry in recent years. Several research groups have studied the application of vanadium in different oxidation states, and they found both +4 and +5 oxidation states of vanadium, that was V(IV) and V(V), were biologically active.⁵⁹⁻⁶¹ However, until that moment there were few reports on structurally characterized vanadium(V) complexes containing amino acid or peptide-like ligands.⁶⁰ In 1993, Crans's group broke the limit as they reported a structural model of vanadium(V)-peptide both in solid-state and solution to reveal the vanadium(V)-protein interactions,⁶¹ where two simple models of complexes, oxovanadium(V) triethanolamine and oxovanadium(V) tri-2-propanolamine, were resolved. The reported distorted trigonal pyramidal vanadium with the nitrogen and the oxo atoms in axial positions demonstrated the ability of vanadium to change the coordination number in environment such as inside the proteins.

Although the current studies with simple oxovanadates complexes have shown significant differences with respect to the affinity of simple oxovanadates for a series of enzymes,⁶² there is still no information presented regarding the interaction between peptides with any of POMs cluster at the molecular level. Therefore, in following they studied the interaction of vanadate decamer cluster and the simple dipeptide glycylglycine (Gly-Gly), which formed a well-defined structure of the compound $(\text{NH}_4)_6(\text{Gly-Gly})_2\text{-V}_{10}\text{O}_{28}\cdot 4\text{H}_2\text{O}$ (abbreviated as **1**).⁵⁸ After the recrystallized Gly-Gly-HCl was added into a rapidly stirred solution of NH_4VO_3 containing hydrochloric acid, a ~ 2 days' incubation resulted in the crystalline material **1**, which was further analyzed by the X-ray crystallography. The detailed cell parameters as atomic coordinates, bond lengths, bond angles, especially the involving hydrogen bonds were supplied in detail in this study. The bond angles and distances observed for the $\text{V}_{10}\text{O}_{28}^{6-}$ unit indicated that the geometry was quite similar to that found in previously reported structures of decavanadatesalts.^{63,64} In addition to the NH_4^+ cations and the associated Gly-Gly units, the unit cell also contained four water molecules, and no disorder involving the water molecules and the ammonium ions occurred in this structure (Fig. 3). The structure of the associated Gly-Gly dipeptide was similar to those assemblies of other zwitterionic amino acids and oligopeptides, which typically exhibited C-O distances of ~ 1.25 Å in carboxylate.^{65,66} The angle of C22-N22-C23 ($119.7(2)^\circ$) was slightly ($\sim 2.5^\circ$) larger than the normal in **1**, while the angle of N22-C23-C24

(113.1(2)°) was slightly smaller (~2°) than the normal, which was the result of the interaction between the Gly-Gly unit and the decavanadate anion. In addition, they found all hydrogen-bonding related protons were located and refined, being good to fully reveal hydrogen bonding patterns and the water molecules and ammonium ions interacted with the decavanadate anion. That was, the structure revealed hydrogen bonding was the controlling factor for the interactions. Each of the ammonium ions forms a hydrogen bond with a doubly bridging oxygen atom of the decavanadate anion; simultaneously the protonated amino terminus of the Gly-Gly dipeptide forms a hydrogen bond to a triply bridging oxygen atom. Due to the hydrogen bonding involving the oxygen atoms of the carboxylate terminus and ammonium ions, the Gly-Gly dipeptide actually linked adjacent decavanadate units. The hydrogen bonding interaction between N21 and O11 indicated the presence of higher electron density on the triply bridging oxygen atom. All the hydrogen bonds in the presented structure were in accord with both experimental and theoretical predictions regarding the basicity of oxygen sites on the vanadate decamer. The hydrogen bonds observed in this structure reflected the flexibility in the Gly-Gly dipeptide in generating hydrogen bonds, and it was most favourable comparing to other reports about the interactions between cations and the oxygen atoms of the decavanadate anion.⁶⁷

In addition, when using the Gly-His to replace Gly-Gly, it formed the compound (NH₄)₂(Gly-His)₄V₁₀O₂₈·16H₂O (**2**). The spectroscopic and elemental analysis found that **2** had a different stoichiometry from **1** due to the overall charge of the dipeptide and its hydrogen-bonding possibility was dependent on the protonation of the imidazole functionality.

Therefore, the Crans's study demonstrated that vanadate decamers can form complexes with peptides through the most basic functionalities and these types of interactions vary significantly with the amino acid sequence and the charge on the protein. They provided the first structural characterizations between oxometalates and peptidic compounds, and paved the way to investigate the self-assembly of peptide and POMs.

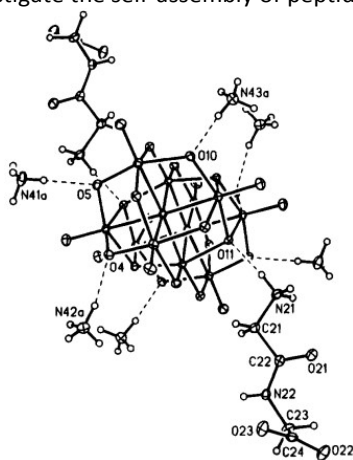


Fig. 3 Drawing of a portion of the structure of **1**. Hydrogen bonds between the polyoxovanadate anion, the cations, and the Gly-Gly zwitterion are indicated by dashed lines.⁵⁸

3.2 Self-assembly of a Keggin-type phosphotungstic acid and a cation diphenylalanine dipeptide.

As the shortest structural recognition motif for the Alzheimer's β -amyloid polypeptide, the cation diphenylalanine peptide (L-Phe-L-Phe, FF) plays a decisive role in the fibril formation, being as an excellent bottom-up building block.⁶⁸ Since G'rbitz *et al.* first found the simple dipeptides can self-assemble into nanotubes, resulting structures have chiral hydrophilic channels with a Van der Waals diameter of up to 10 Å,⁶⁹ the assembly of the FF have attracted many attention. Reches *et al.* demonstrated that FF can self-assemble into well-ordered tubular structures with a long persistence length (100 nm) by a combination of hydrogen bonding and π - π stacking of the aromatic residues.⁷ The FF can also self-assemble into nanofibrils in water by protected 9-fluorenyl-methoxycarbonyl (Fmoc) and thus results in a hydrogel being held together in a network by hydrogen bonding and π - π interaction.^{70,71} In following, the FF dipeptide was found to be capable of self-assembling into individually dispersed and rigid nanowires either in carbon disulfide (CS₂).⁹ In addition, Wang *et al.* discovered the diphenylalanine (Phe-Phe) can form ordered molecular chains on Cu surfaces.⁷²

Almost at the same time, Li *et al.* selected a cationic dipeptide (H-Phe-PheNH₂·HCl) to fabricate nanotubes and the negatively charged nucleic acids could be bound to the tubes and then delivered into cells readily.⁷³ In a further study they found that this cationic dipeptide could assemble into nanotubes at higher concentrations at first, and then these tubular structures can spontaneously be converted into vesicle-like structures at lower concentrations.⁷⁴ Recently, Li's group summarized the self-assembly of the H-Phe-PheNH₂·HCl, and additionally they demonstrated the first assembly of FF with the inorganic compound POMs.

As an important example of self-assembly for POMs and peptides, Li's group studied the self-assembly of cation diphenylalanine peptide FF with a Keggin-type POM, phosphotungstic acid (PTA)H₃PW₁₂O₄₀.⁷⁵ They added PTA to the solution containing FF in a charge ratio of 1:5 at room temperature, and found an immediate, opalescent, cloudy suspension. The analysis on the phenomenon by TEM, SEM and DLS revealed a well-defined, spherical nanostructure with diameters ranging from ~100 to 250 nm (Fig.4). The Fourier transform infrared (FT-IR) spectra of the hybrid colloids indicated PTA and H-Phe-Phe-NH₂·HCl was co-assembled with the strong binding affinity. Meanwhile, they found the assembly of the well-defined spherical structures was determined by the initial concentrations of the peptide and the PTA, as well as their molar ratio. In addition, they investigated for the first time the change in turbidity by varying pH and temperature, and they found the hybrid colloidal spheres were sensitive towards external stimuli such as pH or temperature. By mixing with a variety of guest materials such as hypocrellin B, hydrophilic gold nanoparticles (AuNPs) or fluorescein isothiocyanate with PTA and H-Phe-Phe-NH₂·HCl, the hybrid colloidal spheres displayed an adaptive encapsulation property in the self-assembly process,

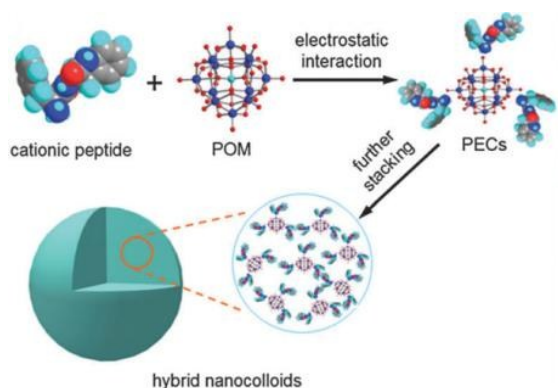


Fig. 4 A schematic illustration of cationic dipeptide and POM co-assembly to hybrid supramolecular structures. The peptide-encapsulated POM clusters were first formed through electrostatic interactions and then such clusters further aggregate into the hybrid spheres.⁷⁵

which opened a new avenue to integrate functional units into self-assembled nanostructures. The adaptive encapsulation of water-soluble molecules can be attributed to the multiple non-covalent interactions between the guest molecules and the peptide-encapsulated clusters (PECs), or to the trapping due to the fast self-assembly of PTA/FF colloidal spheres.^{76,77} Such a flexible organic-inorganic hybrid systems will be useful and typical in the research of co-assemble. And their features will allow them for extensive application of self-assembled nanostructures in controlled release of drugs.

Quit recently, Zhuo *et al.* also introduced the self-assembly of FF@PW12 *via* a re-precipitation strategy.⁷⁸ At first, the supramolecular assemblies of FF and PW₁₂O₄₀ (PW12) in a 3:1 molar ratio were obtained and the aggregates were sub microspheres with average diameters of 520 nm. This self-assembly of PW12 in FF was confirmed using several spectroscopy techniques like UV-vis, FTIR, Raman spectroscopy and NMR, which concluded PW12 and FF were co-assembled into spherical aggregates in water with the electrostatic interaction between them. The chemical structure for the hybrid of (NH₃-PhePhe-COOCH₃)₃PW₁₂O₄₀ (FF₃PW12) with a ratio of 1:3 for PW12:FF was verified by TGA measurements and XRD. In conclusion, they found the building block of (FF)₃PW12 was formed due to electrostatic interactions and then the supramolecular assembly of (FF)₃PW12 occurred *via* non-covalent interactions which undergo two steps self-assembly processes. In addition, they evaluated also the peroxidase-like activities of FF@PW12 and the unique properties which will be introduced in detail as follows.

3.3 Self-assembly of Wells-Dawson-type phosphotungstate and an A β peptide.

Alzheimer's disease (AD) is the most common form of dementia. It is characterized by cerebral extracellular amyloid plaques and intracellular neurofibrillary tangles.⁷⁹ Although the molecular mechanisms of AD pathogenesis were not clearly understood yet owing to its complexity, recent advances have demonstrated that the polymerization of amyloid β -peptides (A β) into amyloid fibrils was crucial.⁸⁰ Qu's group found for the

first time that POMs can inhibit A β aggregation, where they used four different kinds of POMs for comparison and found that the size of POMs played a key role in A β recognition and amyloid inhibition.⁴¹ In following, they combined a Wells-Dawson-type phosphotungstate, K₈[P₂CoW₁₇O₆₁], with a well-known A β -targeted peptide inhibitor, A β 15-20 (Ac-QKLVF-NH₂), to construct the expected hybrids by using straight forward self-assembly approach.⁴⁰ After adding an aqueous solution of K₈[P₂CoW₁₇O₆₁] to a 1,1,1,3,3,3-hexafluoro-2-propanol (HFIP) solution of A β 15-20 at room temperature and 6h incubation, they discovered by SEM the spherical nanoparticles with diameters ranging from about 70 to 100 nm. In addition, the FT-IR spectra of POM@P, POM and A β 15-20 demonstrated strong interactions between POM and peptide. By analysis the X-ray diffraction (XRD) patterns of POM and the hybrid colloidal spheres, they discovered that being similar as POM-dipeptide assembly,⁷⁵ the A β 15-20 molecules can act as analogous to a cationic surfactant, to initially form peptide-encapsulated clusters (PECs) with POMs upon strong electrostatic interactions and following stacked, and finally form supramolecular networks. The further study showed that the initial concentrations of the peptide and the POM as well as their molar ratio will influence the assembly of the well-defined spherical structures; and when the ratio of POM to A β 15-20 was more than 1:2 the colloidal spheres will be cross-linked or aggregated. The unique POM-peptide hybrid particles became more potent against A β 1-40 aggregation which will be introduced in the following part 4.

3.4 Self-assembly of a Lindqvist-type Eu-containing POM with cationic HPV peptides.

Human papillomavirus (HPVs) can easily infect human epithelial cells in the skin and mucosa and have attracted a wide range of attention because of their high hazard to human health.^{81,82} In order to make clear the infection mechanism and the precautionary measures or therapeutic method, researchers have made a lot of effort and found the infection with certain high-risk types is directly associated with anogenital malignancies.⁸³⁻⁸⁵ In a recent research, we studied the interaction of cationic peptides from HPVs capsid proteins with different type of Eu-containing POMs, and discovered the interactions were very interesting.^{86,87} We chose L1 peptides containing 14 amino acids from HPV-18 and -16 L1, HPV16Ctb and HPV18Ctb, which were arginine/lysine-rich ones from high-risk subtypes of HPV major capsid protein. At first, a Lindqvist-type Eu-containing POM, Na₉[EuW₁₀O₃₆]-32H₂O (EuW10) interacting with these two peptides were studied.⁸⁵ When the HPV L1 and EuW10 was mixed at the concentration ratio of 1:1 in the pure water, the well-defined nanoparticles with an average size of ~300 nm were spontaneously formed. The FT-IR spectra illustrated the incorporation of peptide in the assembled nanospheres and the powerful interactions of HPV18Ctb with EuW10. Such interactions of EuW10 and HPV18Ctb, HPV16Ctb were investigated by using fluorescence titration spectra, a much higher luminescence enhancement for HPV18Ctb (35.8-fold) was observed than that for HPV16Ctb

(20.2-fold). The difference in luminescence enhancement suggests a stronger binding ability between EuW10 and HPV18Ctb than HPV16Ctb, which due to the more dispersive surface charges of HPV18Ctb. The Isotherm Titration Calorimetric (ITC) experiment in following gave the binding constants and other thermodynamic parameters between EuW10 and HPV18Ctb/HPV16Ctb in detail, which proved the assembly was completely enthalpy driven. In addition, the influence of temperature on the thermodynamics was detected either by ITC which illustrated both hydrogen bonding and the electrostatic interactions were involved in the EuW10–peptide binding. The following performed Zeta-potential and ^1H NMR measurements confirmed well these results. Further studies in time-resolved fluorescence spectra gave more clearly illustration of the influence of microenvironment to EuW10 when binding with peptides and proved again the strong binding affinity of EuW10 with these peptides.

The method of assembly could be extended to explore the binding of other POMs and peptides, and then we chose a highly charged europium-substituted POM cluster, $\text{K}_{13}[\text{Eu}(\text{SiW}_{10}\text{MoO}_{39})_2] \cdot 28\text{H}_2\text{O}(\text{EuSiWMo})$ in assembling with HPV16Ctb/HPV18Ctb as well as their analogues.⁸⁷ Interestingly, the phenomenon was very different from those of them in binding with EuW10. When the HPV16Ctb was added to the EuSiWMo solution, a two-step assembly and a higher luminescence enhancement (57-fold) was appeared (Fig.5). The time-resolved fluorescence indicated the tighter influence of peptides for the chemical environment of POM cluster perfectly consistent with the luminescence change. In order to clarify the two-step progress, we used ITC measurement to detected the self-assembly, which provided the thermodynamic constants for each step. When the TEM was conducted, we found the EuSiWMo was in a small aggregate even at diluted solution (1.0 μM). With the adding and increasing of HPV16Ctb, we discovered the strip-like aggregates and then bigger spherical assemblies (in step I). Further increasing the HPV16Ctb until the concentration ratio of 3:1, the assemblies to associate and link together while maintaining the spherical morphology (in step II). To further understand the intrinsic mechanism, we analysed the role of the sequence of AAs by using several peptide analogues. The results indicated that both the basic sequence and the length of peptide influences the two-step progress, and the process of step I deal with hydrophobic interactions deriving from the C-termini while the step II involved electrostatic and hydrogen-bonding interactions. It should be noted, the highly charged POMs might bring new interaction forces when binding with peptides or proteins, which have not been taken into consideration in investigations before. Finally, the conclusion was further confirmed through the studied of POMs and SA containing 13 negative charges, which presented a typical two-step process either.²⁸

According to the self-assembly of POMs and HPV L1 peptides, we supplied an easy, cost-effective and efficient fluorescence-enhanced method to detect the positively charged HPV

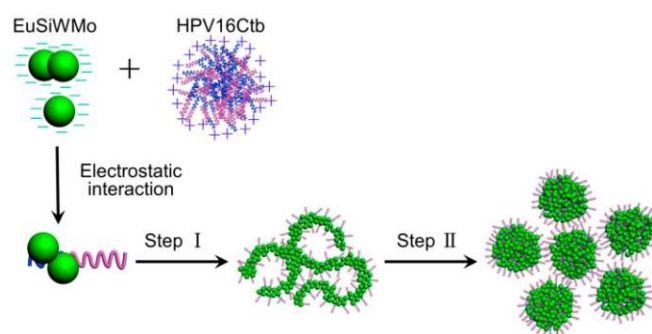


Fig. 5 A schematic binding model and process between EuSiWMo and HPV16Ctb at different molar ratios.⁸⁷

peptides by using an POMs *in vitro* and to discriminate the different subtypes of HPV capsid proteins, which will be introduced in the following part 4.6.^{88,89} Therefore, the study demonstrates both a meaningful preparation for bioinorganic materials and a strategy using POMs to modulate the assembly of peptides and even proteins, which could be extended to other proteins and/or viruses by using the peptides and POMs with similar properties. This strategy could be useful in the future treatment of virus.

3.5 Self-assembly of heteropoly POMs and amphiphilic peptide.

As we all known, multivalent peptide nanofibers have attracted intense attention as promising platforms because these 1D scaffolds offer a high aspect ratio and surface area for the formation of a high-density array of positively charged groups, thus leading to tight binding with negatively charged entities.⁹⁰⁻⁹⁶ Recently, Li *et al.* reported a self-assembly of silica-containing heteropoly $\text{H}_4\text{SiW}_{12}\text{O}_{40}$ (HSiW) with short peptides L1, which consists of an alternating sequence of hydrophilic (lysine) and hydrophobic (azobenzene) residues (Fig.6).⁹⁷ It demonstrated that the multiple electrostatic interactions between them could be utilized to generate multivalent nanofibers. The CD spectra of it demonstrated the commencement of a conformation transition from a random-coil to a β -sheet state.⁹⁸ TEM image presented the uniform nanofibers with a diameter of 12-14 nm and the lengths reaching several micrometers with a molar ratio of 3:1 for L1/HSiW. The hydrophobic and/or π - π interactions lead to the azobenzene units of the ionically self-assembled samples form a densely packed state, which was verified by UV-Vis absorption spectra. In addition, the ITC results implied that the strong electrostatic attraction was the main driving force. High resolution TEM presented a double-layer arrangement which formed by HSiW nanoclusters within the nanofibers with a layer distance of (4~6) nm. Cryogenic TEM and thioflavin T (ThT) titration provided further evidence that long nanofibers with extended β -sheet structures existed in aqueous solution, and that their formation was not caused by the drying effect during the solvent-evaporation process. Zeta-potential measurement revealed that the surface of the nanofibers was covered by highly concentrated positive segments. Then by comparing the molecular length of the β -sheet of L1, the diameter of HSiW, the width of the nanofibers, the distance of the double-layer HSiW and the positive zeta potential, they

found the nanofibers possess a core-shell structure actually. Furthermore, through the comparison to others analogous peptides L2-L7, they found the peptides with less hydrophobic residues were unfavourable for both the one-dimensional (1D) molecular stacking and the stability of the resultant nanostructures. In addition, they also found the strong hydrophobic and/or π - π interactions between the peptides not only facilitate the formation of 1D nanostructures but also improve their stability in water.

These stable nanofibers, as with positively charged surfaces, were multivalent candidates for binding with bacterial cells. By given a series cell experiments using *E. coli* and yeast cells, they found the inhibitory ability of L1 or HSiW alone was poor, while the L1/HSiW nanofibers exhibited significantly enhanced antibacterial efficacy. Then they studied the mechanism by which nanofibers exert their activity through assay for cell viability, and they found that the nanofibers disrupted cell membrane upon contact with *E. coli*. Furthermore, the nanofibers can also resistant the enzyme degradation in human sera. This research not only studied the self-assembly of peptides with POMs but also focused on the enhanced antibacterial activity and related mechanism. It is also expected that the extraordinary properties of POMs by peptide could be used to create hierarchical assemblies for the fields of biological chemistry and materials science.

4. The applications of POM-peptide assembly

The characteristics of the self-assembled particles were uniquely different from the alone peptides or POMs. Meanwhile, the particles possessed advantages in many biochemistry applications, which would be exhibited in detail in following.

4.1 Chiral recognition of hybrid metal oxide by the interaction of peptide and POMs

Chirality in POM chemistry⁹⁹ can be derived from stereogenic arrangement of the achiral subunits in the solid state or in supramolecular assemblies.¹⁰⁰⁻¹⁰² However, it has always been

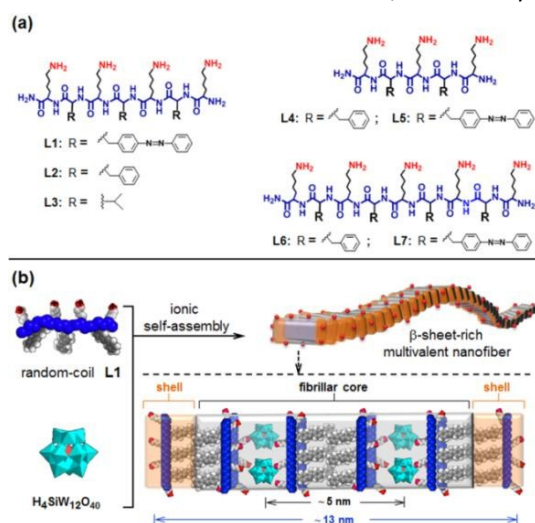


Fig. 6 Ionic self-assembly of peptide L1 and HSiW.⁹⁷

very difficult to recognize the chiral POMs. Early in 2001, Pope *et al.* studied the interactions of $[\alpha\text{-Ce(III)P}_2\text{W}_{17}\text{O}_{61}]^{7-}$ and several amino acids, which presented the diastereomeric arrangements as assayed by ^{31}P NMR spectrum.¹⁰³ In following, Hasenknopf *et al.* observed a strong binding to the organic ligand coupled to additional hydrogen bonds which allowed better chiral sensing of $[\alpha\text{-YbP}_2\text{W}_{17}\text{O}_{61}]^{7-}$, and it was regarded the multiple hydrogen-bonding interactions with organic molecules provided key contribution to direct chiral recognition and resolution.^{104,105} Then, they established an anoxoacyl platform, $(\text{TBA})_6[\alpha\text{-P}_2\text{W}_{17}\text{O}_{61}\{\text{SnCH}_2\text{CH}_2\text{C(=O)}\}]$ (**1**)¹⁰⁶ (TBA = tetran-butyl ammonium), which was a good target for kinetic resolution since its reactive, activated carboxyl moiety could directly attached to the stereogenic POM framework. In addition, the oligopeptides were regarded as good candidates to establish hydrogen bonds with the polyanionic nanocluster as their easily available in both enantiomeric forms. Therefore, in a recent study, in order to accommodate the size of the POM and consequently to increase the odds to achieve chiral recognition of the metal-oxo framework, they chose tripeptides as the organic partners.¹⁰⁷ The desired adduct (**2a**) was obtained and it was isolated together with residual **1**. One of the diastereomers of such the POM conjugated **2a** was formed in slight excess (59/41) as determined by ^1H NMR spectroscopy. Further studies in the different temperature indicated that the lower temperatures led to better selectivity and -40°C allowed the best compromise between selectivity and conversion, which was intrinsically attributed to the lower reactions at cold condition. In addition, they modified amino acids in **1** and found that the extended chains should better wrap around the POM, which was taken place predominantly *via* hydrogen bonding of the peptide to the negatively charged cluster. Finally, they obtained the optimal condition and made sure that the $\text{H}_2\text{N-Trp-Ala-Leu-CO}_2\text{Me}$ was the most promising tripeptide. Actually, the reaction was carried out between racemic **1** and 1 equiv. tripeptide at -40°C for 48h and it delivered about 78% converted POM **2a** in approximately 65/35 diastereomeric ratio, along with 20% recovered **1** (Fig. 7). NMR spectroscopic analysis (including ^1H , ^{31}P and ^{13}C) showed that the single diastereomer was obtained from the reaction of the recovered **1**. Circular dichroism (CD) analysis

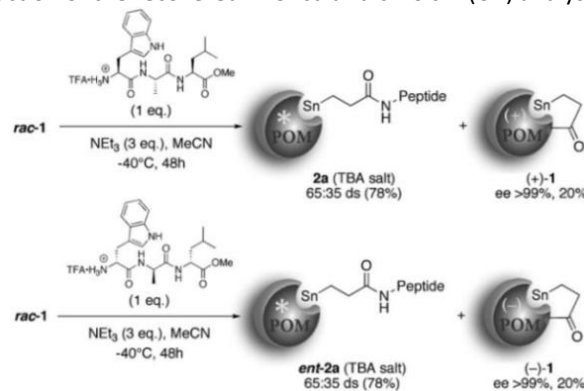


Fig. 7 Kinetic resolution of the enantiomers of α_1 -Dawson POM **1**.¹⁰⁷

further confirmed that they had achieved complete resolution of the enantiomers of **1**.

The molecular recognition of the chiral metal oxide surface of a α 1-substituted Dawson POM enabled its kinetic resolution, which has made possible by the unique properties of organic hybrids of POMs. In addition, the applications of designed chiral hybrids in catalysis (chiral anions), medicinal chemistry, and materials science will be extended more widely in following.

4.2 The promoted hydrolysis of peptide as catalyzed by POMs

The hydrolysis of the peptide at specific bond was one of the most important and necessary procedures in biotechnology. There were numerous studied focused on the cleavage of protein or peptide.¹⁰⁸ However, both they suffered from serious shortcomings, such as too many possible sites by using proteolytic enzymes and the harsh conditions for chemical reagents. Several metal ions,¹⁰⁹⁻¹¹³ including Pd(II), Pt(II), Ni(II), Zr(IV), Co(III), and Ce(IV) have been reported to promote the hydrolytic cleavage of inactivated amide bonds in peptides and proteins, while the use of metal complex in this field was still scare reported for many years. However, the research group of Tatjana broke the limit; they reported several good investigations on the hydrolysis of peptide catalysed by metal complex. For example, the first promoted cleavage of hydrolytic peptide was achieved by a negatively charged $[\text{MoO}_4]^{2-}$ oxyanion,¹¹⁴ which was attributed to its ability to efficiently coordinate to the X-Ser peptides. Such an coordination polarized their carbonyl group toward the internal nucleophilic attack by the hydroxyl group in Ser residue. Then, they reported the incorporation of Zr(IV) into the Wells-Dawson POM and gave the first example of phosphoester bond hydrolysis in 4-nitrophenyl phosphate (NPP) and bis-4-nitrophenyl phosphate (BNPP), two commonly used DNA model substrates. Promoted result was obtained by metal-substituted POMs, which resulted in a catalyst for the homogeneous hydrolysis of phosphoester bond hydrolysis.¹¹⁵ The study inspired them to extend the use of POMs as artificial phosphoesterases by incorporating metal ions into hetero POMs.

In a recent study, they make use of the polyoxometalate complex, $\text{Zr}(\alpha_2\text{-P}_2\text{W}_{17}\text{O}_{61})_2$, to explore the cleavage on peptide, and gave the first example of peptide hydrolysis as catalysed by the Zr(IV)-substituted Wells-Dawson type polyoxometalate.¹¹⁶ They synthesized a series of metal-substituted Wells-Dawson POMs and examined their hydrolytic activity toward the peptide bond in glycyl-glycine (GG). They found that the Zr(IV)- and Hf(IV)-substituted ones were the most active, and they selected Zr(IV)-substituted Wells-Dawson POM, $\text{K}_{15}\text{H}[\text{Zr}(\alpha_2\text{-P}_2\text{W}_{17}\text{O}_{61})_2] \cdot 25\text{H}_2\text{O}$ (**1**), to study the catalysis of hydrolysis in detail. First, they studied the behaviour of **1** in aqueous solution and found the Zr(IV) showing higher coordination numbers in comparison to other transition metal ions which were usually tetra- or hexa-coordinated. Then they found the GG was fully hydrolysed to glycine (G) in the presence of equimolar amounts of **1** at pD5.0 and 60 °C, provided the corresponding rate constant (K_{obs}) for

the hydrolysis. The rate constant of hydrolysis represents a significant acceleration compared to the blank reaction in which no hydrolysis was observed after several months under the same reaction conditions. In following, they investigated the hydrolysis of Gly-Gly derivatives, which were modified at the N- and C-terminal end. The ^1H NMR spectra of these derivatives demonstrated the free amino terminus were important for the interaction of the peptide with the POM. Further studies on the binding of **1** to GG were performed by ^{13}C NMR, and the largest shift being observed for the amide carbonyl. These large chemical shift values of GG manifested it was the coordination of the amide carbonyl to Zr(IV) that facilitated amide bond hydrolysis *via* activating the amide carbon toward nucleophilic attack by water molecules, which was consistent with the derivatives test. In addition, the hydrolysis of GG in the presence of several non-reactive substrate analogues was also examined, such as oxalic acid, malonic acid, succinic acid, glutamic acid and so on. The different inhibition for the hydrolysis of GG indicated that carbonyl groups bind efficiently to the Zr(IV) centre in **1**, suggesting the coordination of GG to **1** and its activation toward nucleophilic attack was mainly governed by carbonyl group interaction. Finally, they concluded the hydrolysis mechanism and found coordination of the amide carbonyl leads to Lewis acid activation of the amide bond and made it more susceptible toward nucleophilic attacked by water (Fig.8 and 9). Both the attack of coordinated water, solvent water and the according mechanisms were kinetically indistinguishable.¹⁰⁹ Especially, the N-terminal amine group was considered as the second coordinating entity, which explained well why the peptide as the N-blocked analogue, acetamidoglycylglycinate (AcGG), was not hydrolyzed in the presence of **1**. Then other dipeptides were fully hydrolyzed by **1** finally.

Later on, they studied a series of dipeptide as catalyzed by a zirconium(IV)-substituted Lindqvist-type POM, $(\text{Me}_4\text{N})_2[\text{W}_5\text{O}_{18}\text{Zr}(\text{H}_2\text{O})_3]$ (ZrW5)¹¹⁷ and also promoted the detailed kinetic of Zr(IV)-substituted Keggin type polyoxometalate with dipeptide.¹¹⁸ They found this Zr^{IV}-substituted POM was shown to be more active in the hydrolysis of inert amide bonds of series dipeptides under homogeneous reaction conditions. Among the dipeptides examined, those with the X-Ser amino acid sequence were

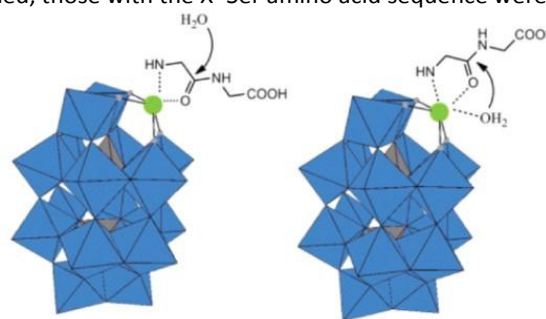


Fig. 8 Mechanism for the hydrolysis of GG in the presence of **1**: nucleophilic attack of solvent water (Left) and coordinated water (Right).¹¹⁶

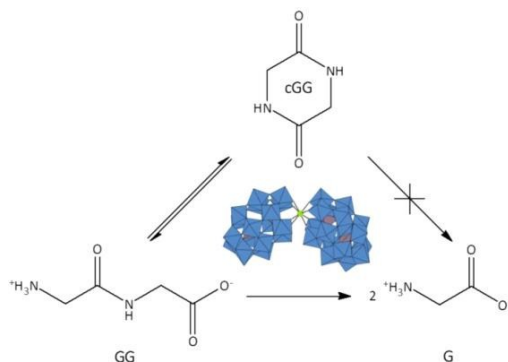


Fig. 9 Hydrolysis of GG in the Presence of **1**.¹¹⁶

hydrolyzed most effectively because of a N→O acyl rearrangement. And the hydrolysis was faster than that of dipeptides containing aliphatic side chains, and the fastest hydrolysis was observed for His–Ser peptide. Then, they also investigated the selective hydrolysis of HSA¹¹⁹ and Lysozyme⁴⁶ by POM complexes, and promoted the hydrolysis mechanism that the coordination of the peptide to Zr(IV) leads to polarization of the peptide carbonyl group facilitating its hydrolysis, which was basing on the hydrolysing of short peptides.

In following, with a series of Zr(IV)-substituted POMs studies, they found that Zr(IV)-substituted Lindqvist-, Keggin-, and Wells–Dawson-type POMs selectively hydrolyze the protein myoglobin at Asp-X site under mildly acidic and neutral conditions, which was the first example of highly sequence selective protein hydrolysis by POMs.¹²⁰ In addition, they also found that a polypeptide with 30 amino acids, oxidized insulin chain B, being selectively cleaved by the Zr(IV)-substituted Wells–Dawson POM, $K_{15}H[Zr(\alpha_2-P_2W_{17}O_{61})_2] \cdot 25H_2O$, under physiological pH and temperature in aqueous solution. Such study was the first report on the selective hydrolysis of a polypeptide system by a metal-substituted POM.¹²¹ Recently, the interaction between $K_{15}H[Zr(\alpha_2-P_2W_{17}O_{61})_2]$ and a range of surfactants were studied in detail by ¹H, ¹³C, and ³¹P NMR, ¹H diffusion-ordered NMR (¹H DOSY), and nuclear Overhauser effect spectroscopy (NOESY).¹²² They found that the cationic surfactant cetyl(trimethyl)ammonium bromide (CTAB) caused precipitation of $K_{15}H[Zr(\alpha_2-P_2W_{17}O_{61})_2]$ due to strong electrostatic interactions, while the anionic sodium dodecyl sulfate (SDS) and neutral Triton X-100 (TX-100) surfactants did not exhibit any interaction at neutral pH solutions. Most importantly, in the presence of anionic, neutral, and zwitterionic surfactants, $[Zr(\alpha_2-P_2W_{17}O_{61})_2]^{16-}$ preserved its catalytic activity towards the hydrolysis of peptide bonds. This study was a first and important step in developing Zr^{IV}-substituted POMs as artificial metallopeptidases that are active in surfactant solutions. All the results together indicated that the interaction between peptides and POMs by weak force was very important in the catalytic process. It has been extensively applied to the study of biological properties for POMs and will light on the molecular origin of their biological activity.

4.3 Enhanced Inhibition of Aβ aggregation

As a progressive neurodegenerative disorder, AD is characterized by the deficits in the cholinergic system and deposition of beta amyloid in the form of neurofibrillary tangles and amyloid plaques. It is the most common form of dementia, which afflicts more than 24 million people worldwide.¹²³ A significant body of data has indicated that the polymerization of amyloid-β (Aβ) peptide into amyloid fibrils is a critical step in the pathogenesis of AD.^{124–128} Therefore, inhibition of Aβ aggregation has been considered as an attractive therapeutic and preventive strategy for AD treatment. As it well known, peptides containing the recognition residues, KLVFF, have been shown to bind the homologous sequence in Aβ40 or Aβ42 and disrupt their aggregation. So Qu's group utilized the unique properties of POMs and Aβ16–20 to self-assemble the hybrid particles of POM-peptide (POM@P, here P is Aβ16–20), which was further used as bio-functional Aβ inhibitors (Fig.10).⁴⁰ Firstly, by using straightforward self-assembly approach, they combined a Wells-Dawson-type phosphotungstate, $K_8[P_2CoW_{17}O_{61}]$, with the Aβ-targeted peptide inhibitor Aβ15–20 (Ac-QKLVFF-NH₂),¹²⁹ to self-assemble the expected hybrids. Then they investigated the inhibition activity of these novel nanoparticles in Aβ aggregate formation by using a widely used thioflavin T (ThT) fluorescence assay.¹³⁰ They discovered that a 2:1 ratio of Aβ1–40 to POM@P (here P is Aβ 15–20, and the ratio of POM/Aβ15–20 is 1:2) inhibited the relative change of ThT fluorescence by more than 65%; whereas the same amount of POM or Aβ 15–20 inhibited ThT only by 35% or 45%, respectively. So, in comparison to POM or Aβ15–20 alone, the two-in-one bifunctional POM@P nanoparticles showed enhanced targeting inhibition effect. In addition, the PC12 cells was employed to detect whether the nanoparticles could be used to block Aβ1–40-mediated cellular toxicity by 3-(4,5-dimethylthiazol-2-yl)-2,5-diphenyltetrazolium bromide(MTT) assay. They found that the Aβ fibrils (10 μM) led to a decrease of 46% in cellular reduction of MTT. Treatment of the cells with Aβ in the presence of POM@P (6 μM) increased the survival of the cells to about 82% and POM@P

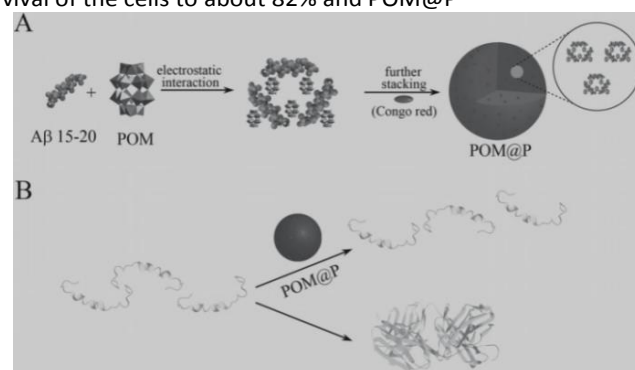


Fig.10 Schematic representation of the peptide-POM conjugates used for AD treatment. (A) The schematic illustration of self-assembly of Aβ15–20 and POM to hybrid spheres. (B) The assembled peptide and POM nanoparticles can effectively inhibit Aβ1–40 aggregation.⁴⁰

nanoparticles themselves were nontoxic under the same conditions. In particular, by incorporating a clinical-used A β fibril specific staining dye Congo red (CR) into POM@P nanoparticles they found it was possible to monitor the A β morphology changes in real time according to CR fluorescence change, and consequently the nanoparticles could act as effective fluorescent probes to monitor the inhibition process of POM@P. Therefore, the self-assembled POM-A β in targeting peptide-CR hybrids possessed obviously enhanced inhibition efficiency and real-time monitoring in one system,¹³¹ which promoted the design of multifunctional targeting agents for AD treatment. In addition, the enhanced inhibition efficiency and specific ability targeted-A β have been considered important and useful in clinical treatment, as with reduced side effects of POM. Furthermore, these methods are easily compared with others which are too complicated, expensive, time consuming and difficult to get large-scale production for extensively use.

4.4 Drug delivery

It has found that the POMs exhibit excellent photo luminescent properties.^{26,132} When the POMs was encapsulated by poly-acrylic acids (PAA) in aqueous solutions, the stability of POM would be enhanced. Especially, it can promote biocompatibility of POM-based nanomaterials and provide enriched carboxyl groups for subsequent bio-conjugation with a mitochondria-targeting peptide.²⁶ Recently, Zhang *et al.*¹³³ reported an important new understanding of the interactions between nanoparticles and cells by using Na₉EuW₁₀O₃₆·32H₂O (EuW10), acrylic acids (AA) and a positively-charged peptide (Dmt-D-Arg-Phe-Lys-NH₂)¹³⁴ (Fig.11). First, they prepared the EuW10@PAA (polymerized acrylic acids) nanoparticles by adding EuW10 into acrylic acid with ammonium persulfate (APS) as the initiator to synthesize PAA in aqueous solutions. The mixture was managed again to obtain purified EuW10@PAA nanoparticles, which enhanced the fluorescence of EuW10 by reducing the quenching effect of water molecules and promoted simultaneously the biocompatibility of POM-based nanomaterials.²⁶ The diameters of the nanoparticles were proven to be approximately 60 nm by TEM. In subsequent, the peptide in targeting mitochondria was covalently conjugated onto the carboxyl-functionalized EuW10@PAA nanoparticles and finally formed peptide-conjugated nanoparticle (NP-peptide). Both the bare NP and NP-peptide were assayed and compared in the MALDI-TOF mass spectrometry, which suggested successful coupling of the peptides on NP surface. They also tested the cytotoxicity of the nanoparticles by using MTT assays and the dual-colour staining experiments with dye molecules of calcein-AM and propidium iodide (PI), which suggested that the NP-peptide exhibited low cytotoxicity during the incubation with the MCF-7 cells, due to good encapsulation with PAA molecules. Then, by comparing the intracellular distribution of EuW10 nanoparticles with or without surface modification of peptides by confocal laser scanning microscopy (CLSM), they found the NP-peptide can be uptake by MCF-7 cells and delivered to mitochondrial significantly higher than bare EuW10 nanoparticles. Thus, it

demonstrated the prominent effect of surface modification of nanoparticles on their intracellular distribution. In addition, they also investigated the intracellular trafficking behaviours of NP-peptide in a dynamic mode, revealing interesting dynamics in the translocation of NP-peptide from mitochondria to lysosomes in a time-dependent manner (Fig. 12). It displayed a significant increase of the signals overlapping (triplex) between NP-peptide, mitochondria and lysosomes at the later stage. In addition, they further investigated the phenomenon and the related molecular mechanism by using Parkin, a protein recruited due to the changes of mitochondria membrane potential. The experiments supported that Parkin was likely mediating this autophagic degradation associated with the change of mitochondrial membrane potential. The results also confirmed that the damages of mitochondrial membrane potential induced by NP-peptide and supported the molecular mediation by Parkin in the mitophagy. Further, these biological effects induced by NP-peptide can reciprocally affect the distribution patterns and the fates of nanoparticles in the cell metabolism by providing an alternative route of intracellular trafficking. These new understanding of the mutual activities between nanoparticles and cells lay the foundation for biosafety evaluation of nanoparticles and would be critical important for study of the drug delievery.¹³³

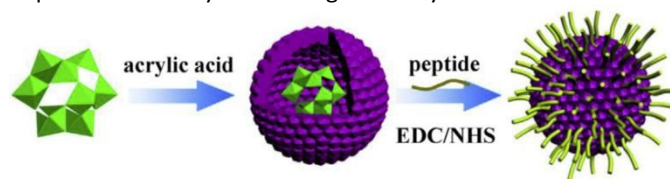


Fig.11 Schematic illustration of the synthesis of EuW10@PAA nanoparticles and subsequent bioconjugation with peptides.¹³³

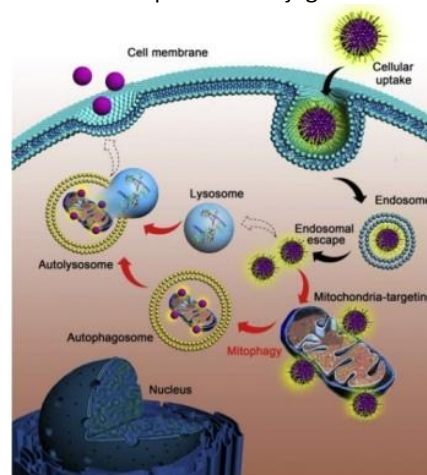


Fig. 12 Schematic illustration of intracellular trafficking dynamics of mitochondria targeting nanoparticles. Mitophagy is induced by NP-peptide, involving the formation of auto phagosomes and their subsequent fusion with lysosomes (autolysosomes); these steps hosted by the cell reciprocally change the fate of NP-peptide in cell metabolism through an alternative intracellular trafficking route.¹³³

4.5 Enhancement of peroxidase-like performance

There were several reports introduced the self-assembly of diphenylalanine peptide and POMs,^{39,75} which indicated that the introduction of POMs indeed enhanced the biocompatibility of the hybrids constructed from FF and cationic ions.¹³⁵⁻¹³⁷ Recently, Zhuo *et al* studied the assembly behaviour and characterization of FF and H₃PW₁₂O₄₀ (PW12) nanospheres in the process of H₂O₂ hydrolysis.¹³⁸

As we all known the detection of H₂O₂ has attracted much attention as its production affects many biochemistry reactions in the body that are critical for human health.¹³⁹⁻¹⁴¹

The common method to catalyse H₂O₂ hydrolysis involves the use of horseradish peroxidase (HRP) by optical detection strategy, which was effective company inherent drawbacks including the sensitivity of catalytic activity to environmental changes and low operational stability with time consuming and expensive preparation.¹⁴²⁻¹⁴⁴ POMs have been shown to demonstrate enzyme mimetic activity and Wang *et al.* have found that PW12 exhibited intrinsic peroxidase-like activity and its catalysis was strongly dependent on pH, temperature and H₂O₂ concentration,¹⁴⁵ However, pristine POMs catalyse the reaction in a homogeneous way, causing recovery and contamination issues and was very stringent in bio-detection demand.

Before this publication, Qu's group have found that the carboxyl(-COOH) modified graphene oxide (GO) could catalyze 3,3',5,5'-tetramethylbenzidine (TMB) to produce a blue-coloured product in the presence of H₂O₂.¹⁴⁶ Then, a super lattice monolayer containing POMs on GO showed enhanced photo electrochemical properties being ascribable to the synergistic effects between the super lattice and GO.¹⁴⁷

At first, they formed the spherical structures of FF@PW12 being introduced before. Then they evaluated the peroxidase-like activities of FF@PW12. The catalysis of peroxidase on substrate TMB was examined in the presence of H₂O₂ with FF@PW12 hybrid and other controls for comparison. They found the reaction system of TMB/H₂O₂/FF@PW12 was stable for a long aging time, in which no agglomeration was observed throughout the process. Meanwhile, the relative activity was ~13 times higher than that of pristine PW12 without any capping agents under similar reaction conditions. After that, they further constructed the FF@PW12@GO composite and the spherical structures of FF@PW12 were maintained on the surface of GO oxide (Fig. 13). The average size of the

Sub-microspheres was about 480 nm, indicating the confinement effect of GO on the spherical growth. Raman results indicated the successful integration of the spheres and GO. They firstly investigated the peroxidase-like activity as a function of GO contents in the composite and found the peroxidase-like activity of the FF@PW12@GO (5 wt %) composite indeed exhibits higher absorbance in 10 min than that of FF@PW12. The relative performance of FF@PW12@GO is ~1.7 times higher than that of FF@PW12 and the catalytic activity of FF@PW12@GO is much higher in acidic media than in neutral conditions. Then they analysed the mechanism of the catalysis property of FF@PW12@GO, and found two steps were involved in the oxidation reaction of TMB. H₂O₂ molecules were first adsorbed to FF@PW12@GO and then get activated by the synergistic effects of the three components. Furthermore, less •OH radical was generated in the former case, being consistent with the difference of peroxidase-like activities of these two systems. Therefore, Zhao *et al.* conducted a ternary hybrid FF@PW12@GO based on the self-assembly of FF@PW12 on GO and found an excellent peroxidase-like mimic, which exhibited enhanced peroxidase-like activity. This co-assembly method based on peptides and POMs opens up a promising route in constructing heterogeneous peroxidase-like mimics through the use of POMs *via* the introduction of GO for building the H₂O₂ sensors.

4.6 Detection and discrimination of HPV capsid proteins

We have reported the self-assembly of HPV capsid peptides with Eu-containing POMs, which induced large luminescence enhancement of Eu(III). The related mechanism investigation revealed the enhanced magnitude was determined both by the number and sequence of basic amino acids (AAs) in the peptide, which supplied the possibility to detect and discriminate the related capsid proteins enriched basic AAs.

At first, we added a peptide from the C-terminal of the major capsid protein of HPV16, HPV16L1Ctb, to the buffer solution containing EuW10 and the luminescence changes presented a linear increasing in a wider range, which was attributed to the strong binding between EuW10 and HPV16L1Ctb.⁸⁸ Then the luminescence intensity reached its maximum when the concentration of peptides increased up to 120 μM, and then it became stable. Such results illustrated that the enhanced luminescence response of EuW10 to basic peptide would be useful to detect the capsid proteins of HPV L1 and/or L2, as several typical cationic peptides are involved there.

Then we detected and compared the L1 peptidic segments from HPV capsid protein, HPV16L1Cta and HPV16L1Ctb, each contained six basic residues. It was found the luminescence intensity of POM induced by HPV16L1Cta were relatively stronger at low concentration, while it was much less efficient at higher concentrations than those of HPV16L1Ctb. The different level of luminescence enhancement of EuW10 induced by them may be attributed to the polybasic residues (KRKRRK) in HPV16L1Ctb, which had been suggested to have higher compatibility and binding affinity to another POM, EuSiWMo.⁸⁷ By using the identical method, we analysed others two Arg/Lys-rich cationic peptides from minor capsid protein

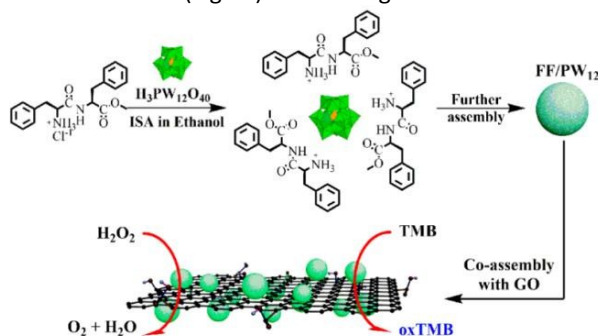


Fig. 13 Schematic illustration of the assembly process of the FF@PW12@GO complex.¹³⁸

L2, HPV16L2Ct and HPV16L2Nt, either. The different luminescence changes between them illustrated in addition to the dominant electrostatic interaction between them other factors as the distinction of K and R proportions in the peptides should also be considered. In addition, through series experiments of ITC, we discovered the different binding constants of the POMs with four peptides, companying with the large difference of EuW10 luminescence enhancement induced by them should be extended to peptides from other subtypes of HPV capsid protein.

Further, we found the luminescence intensity was enhanced and indicated the EuW10 could also be used to detect the L1 pentamers. At first, HPV16 L1 protein was detected in MES-NaOH buffer solution and the additions of it into the POM solution induced luminescence enhancement with the limit-of-detection (LOD) was 0.5 mM. When it was used to detect another high-risk subtype of HPV, HPV58 L1, we found it could induce the luminescence change either and showed similar but stronger enhancement than HPV16 L1. This illustrated the universality for the binding of EuW10 with the recombinant HPV L1 protein from *E. coli*. Such an approach could be extended to detect other HPV subtypes and/or even other kinds of proteins with identical properties. In summary, the self-assembly of Arg/Lys-rich cationic peptides from HPV capsid protein and EuW10 provided a good support to detect the representative peptides and HPV capsid protein *in vitro*, which opened a way to develop an easy-to-perform, cost-effective and efficient method to detect HPV capsid proteins, and would be improved by using more appropriate and/or sensitive protein as well as to discriminate different subtype of HPV by using POMs as probes.

After that, the POMs was also used to discriminate HPVs in different subtypes.⁸⁹ We chose four peptides, HPV44Ctb, HPV16Ctb, HPV18Ctb and HPV5Ctb, from the sequences of different HPV subtypes. At first, the fluorescence spectra of EuSiWMO and [Eu(PW₁₁O₃₉)²⁻]¹¹⁻ (EuPW11), possessing 13 and 11 negative charges respectively, were detected when binding with these peptides; however, neither could be discriminated well because of too strong binding affinity between POM and peptide. Then, the EuW10, which contained less negative charges of 9, was proposed to further discriminate the virus capsid proteins between different HPV subtypes. The differences of luminescence responses confirmed EuW10 was a suitable POM to differentiate them. The discrimination mechanisms between them were then revealed by time-resolved fluorescence spectra and ITC in detail, which indicated it was efficiently important for EuW10 with a moderated binding affinity ($K_b = 10^5\text{--}10^6 \text{ M}^{-1}$) when recognizing the peptides. The strong-dependences of luminescence enhancement of POM both on the number and sequences of basic AAs in peptide was revealed well in the present study, which were further verified by other two peptides of HPV16Ctb1 and HPV16Ctb2. Therefore, this study reported a simple, low-cost and efficient fluorescence enhanced method to discriminate peptides from different subtypes of HPV capsid proteins.

In summary, these part results supplied an excellent application of the type of inorganic materials, polyoxometalate, in virus science, and might be helpful to explore the mechanism of virus infection.

Conclusion and Perspectives

With the explosion of the number of new studies on POM-peptide interactions, a very exciting era in bio-related application of POMs is coming. Further development of novel POM-peptide interactions is also closely dependent on the better understanding of the mechanism of POMs-protein recognitions, which will further extend accesses to a wide variety of inorganic groups on the POMs to meet specific requirements in biological applications.

In the past years, the self-assembly of POMs and biomolecules like protein and peptide have attracted broad attention as their unique properties. For example, the self-assemble of POM and A β peptide can be efficiently used to refrain the aggregation of A β as an inhibitor. We believe that the self-assembly of peptides and POMs will open a new field for the study of inorganic medicines, which will be a great improvement to prevent and treat many diseases like HIV and AD. We also believe that a better understanding of the self-assemble mechanism will no doubt help in judicious design and improve the function of highly efficient POM-based materials. Therefore, it is very critical to make use of different techniques and methodologies to drive POM@peptide chemistry forward, and in this respect, we hope can learn much from this interdisciplinary science.

Acknowledgements

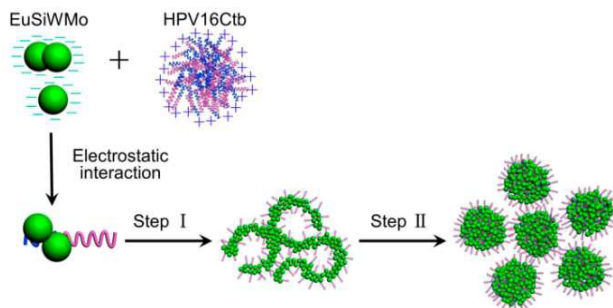
We greatly appreciate the financial support from the projects of NSFC (Nos. 21373101 and 91027027) and the State Key Laboratory of Supramolecular Structure and Materials, Jilin University.

References

- 1 Y. Mai, A. Eisenberg, *Chem. Soc. Rev.*, 2012, **41**, 5969–5985.
- 2 S. Chen, P. Slattum, C. Wang, L. Zang, *Chem. Rev.*, 2015, **115**, 11967–11998.
- 3 J.-M. Lehn, *Proc. Natl. Acad. Sci. USA*, 2002, **99**, 4763–4768.
- 4 G. M. Whitesides, B. Grzybowski, *Science*, 2002, **295**, 2418–2421.
- 5 K. Rajagopal, J. P. Schneider, *Curr. Opin. Struct. Biol.*, 2004, **14**, 480–486.
- 6 D. de la Rica, H. Matsui, *Chem. Soc. Rev.*, 2010, **39**, 3499–509.
- 7 M. Reches, E. Gazit, *Science*, 2003, **300**, 625–627.
- 8 I. W. Hamley, *Angew. Chem., Int. Ed.*, 2007, **46**, 8128–8147.
- 9 T. H. Han, J. Kim, J. S. Park, C. B. Park, H. Ihee, S. O. Kim, *Adv. Mater.*, 2007, **19**, 3924–3927.
- 10 L. Adler-Abramovich, M. Reches, V. L. Sedman, S. Allen, S. J. B. Tandler, E. Gazit, *Langmuir*, 2006, **22**, 1313–1320.
- 11 J. Ryu, C. B. Park, *Adv. Mater.*, 2008, **20**, 3754–3758.
- 12 E. Gazit, *Chem. Soc. Rev.*, 2007, **36**, 1263–1269.
- 13 L. Niu, X. Chen, S. Allen, S. J. B. Tandler, *Langmuir*, 2007, **23**, 7443–7446.

- 14 A. Proust, R. Thouvenot, P. Gouzerh, *Chem. Commun.*, 2008, 1837–1852.
- 15 I. V. Kozhevnikov, *Chem. Rev.* 1998, **98**, 171–198.
- 16 M. T. Pope, A. Muller, *Angew. Chem., Int. Ed.*, 1991, **30**, 34–48.
- 17 D.-L. Long, E. Burkholder, L. Cronin, *Chem. Soc. Rev.*, 2007, **36**, 105–121.
- 18 E. Coronado, C. Gimenez-Saiz, C. J. Gomez-Garcia, *Coord. Chem. Rev.*, 2005, **249**, 1776–1796.
- 19 T. Liu, E. Diemann, H. Li, A. W. M. Dress, A. Muller, *Nature*, 2003, **426**, 59–62.
- 20 P. Burton-Pye, L. C. Francesconi, *Dalton Trans.*, 2011, **40**, 4421–4433.
- 21 D. Drewes, E. M. Limanski, B. Krebs, *Dalton Trans.*, 2004, 2087–2091.
- 22 L. Zheng, Y. Ma, G. Zhang, J. Yao, B. Keita, L. Nadjo, *Phys. Chem. Chem. Phys.*, 2010, **12**, 1299–1304.
- 23 L. Zheng, Z. Gu, Y. Ma, G. Zhang, J. Yao, B. Keita, L. Nadjo, *J. Biol. Inorg. Chem.*, 2010, **15**, 1079–1085.
- 24 G. Hungerford, K. Suhling, M. Green, *Photochem. Photobiol. Sci.*, 2008, **7**, 734–737.
- 25 G. Hungerford, F. Hussain, G. R. Patzke, M. Green, *Phys. Chem. Chem. Phys.*, 2010, **12**, 7266–7275.
- 26 J. Zhang, Y. Liu, Y. Li, H. Zhao, X. Wan, *Angew. Chem. Int. Ed.*, 2012, **51**, 4598–4602.
- 27 H.-W. Li, Y. Wang, T. Zhang, Y. Wu, L. Wu, *ChemPlusChem.*, 2014, **79**, 1208–1213.
- 28 P.-F. Gao, S. Zhang, H.-W. Li, T. Zhang, Y. Wu, L. Wu, *Langmuir*, 2015, **31**, 10888–10896.
- 29 H. N. Miras, J. Yan, D. L. Long, L. Cronin, *Chem. Soc. Rev.* 2012, **41**, 7403–7430.
- 30 D. Y. Du, J. S. Qin, S.-L. Li, Z. M. Su, Y. Q. Lan, *Chem. Soc. Rev.*, 2014, **43**, 4615–4632.
- 31 T. Yamase, *J. Mater. Chem.*, 2005, **15**, 4773–4782.
- 32 H. Stephan, M. Kubeil, F. Emmerling, C. E. Miller, *Eur. J. Inorg. Chem.*, 2013, 1585–1594.
- 33 G. Liu, T. Liu, *J. Am. Chem. Soc.*, 2005, **127**, 6942–6943.
- 34 C. Lin, W. Zhu, H. Yang, Q. An, C. Tao, W. Li, J. Cui, Z. Li, G. Li, *Angew. Chem., Int. Ed.*, 2011, **50**, 4947–4951.
- 35 I. W. Hamley, M. J. Krysmann, V. Castelletto, L. Noirez, *Adv. Mater.*, 2008, **20**, 4394–4397.
- 36 J. Wang, X. Mi, H. Guan, X. Wang, Y. Wu, *Chem. Commun.*, 2011, **47**, 2940–2942.
- 37 K. Ariga, J. P. Hill, Q. M. Ji, *Phys. Chem. Chem. Phys.*, 2007, **9**, 2319–2340.
- 38 C. S. Peyratout, L. Daehne, *Angew. Chem., Int. Ed.*, 2004, **43**, 3762–3783.
- 39 X. Yan, P. Zhua, J. Li, *Chem. Soc. Rev.*, 2010, **39**, 1877–1890.
- 40 M. Li, C. Xu, L. Wu, J. Ren, E. Wang, X. Qu, *Small*, 2013, **9**, 3455–3461.
- 41 J. Geng, M. Li, J. Ren, E. Wang, X. Qu, *Angew. Chem.*, 2011, **123**, 4270–4274.
- 42 J. T. Rhule, C. L. Hill, D. A. Judd, R. F. Schinazi, *Chem. Rev.*, 1998, **98**, 327–357.
- 43 D. A. Judd, J. H. Nettles, N. Nevins, J. P. Snyder, D. C. Liotta, J. Tang, J. Ermolieff, R. F. Schinazi, C. L. Hill, *J. Am. Chem. Soc.*, 2001, **123**, 886–897.
- 44 H. Yu, M. Li, G. Liu, J. Geng, J. Wang, J. Ren, C. Zhao, X. Qu, *Chem. Sci.*, 2012, **3**, 3145–3153.
- 45 Y.-F. Song, R. Tsunashima, *Chem. Soc. Rev.*, 2012, **41**, 7384–7402.
- 46 K. Stroobants, E. Moelants, H. G. T. Ly, P. Proost, K. Bartik, T. N. Parac-Vogt, *Chem. Eur. J.*, 2013, **19**, 2848–2858.
- 47 G. J. Zhang, B. Keita, C. T. Craescu, S. Miron, P. D. Oliveira, L. Nadjo, *J. Phys. Chem. B*, 2007, **111**, 11253–11259.
- 48 G. J. Zhang, B. Keita, J. C. Brochon, P. D. Oliveira, L. Nadjo, C. T. Craescu, S. Miron, *J. Phys. Chem. B*, 2007, **111**, 1809–1814.
- 49 L. Nadjo, *Biomacromolecules*, 2008, **9**, 812–817.
- 50 L. Zheng, Z. Gu, Y. Ma, G. Zhang, J. Yao, B. Keita, L. Nadjo, *J. Biol. Inorg. Chem.*, 2010, **15**, 1079–1085.
- 51 V. Goovaerts, K. Stroobants, G. Absillis, T. N. Parac-Vogt, *Phys. Chem. Chem. Phys.* 2013, **15**, 18378–18387.
- 52 V. Goovaerts, K. Stroobants, G. Absillis, T. N. Parac-Vogt, *Inorganics* 2015, **3**, 230–245.
- 53 F. Xin, M. T. Pope, *J. Am. Chem. Soc.*, 1996, **118**, 7731–7736.
- 54 J. Liu, J. Peng, E. Wang, L. Bi, S. Guo, *J. Mol. Struct.*, 2000, **525**, 71–77.
- 55 R. Y. Wang, D. Z. Jia, L. Zhang, L. Liu, Z. P. Guo, B. Q. Li, J. X. Wang, *Adv. Funct. Mater.*, 2006, **16**, 687–692.
- 56 R. Y. Wang, L. Liu, D. Z. Jia, J. M. Luo, Z. T. Fan, *Chem. J. Chin. Univ.* 2004, **25**, 2208.
- 57 Y. Kong, L. Pan, J. Peng, B. Xue, J. Lu, B. Dong, *Mater. Lett.*, 2007, **61**, 2393–2397.
- 58 D. C. Crans, M. Mahroof-Tahir, O. P. Anderson, M. M. Miller, *Inorg. Chem.*, 1994, **33**, 5586–5590.
- 59 D. Rehder, *Angew. Chem., Int. Ed. Engl.*, 1991, **30**, 148–167.
- 60 O. T. Colpas, J. D. Haschele, J. Kampf, V. L. Pmraro, *J. Am. Chem. Soc.*, 1992, **114**, 9925–9933.
- 61 D. C. Crans, H. Chen, O. P. Anderson, M. M. Miller, *J. Am. Chem. Soc.*, 1993, **115**, 6769–6776.
- 62 D. C. Crans, *Comments Inorg. Chem.*, 1994, **16**, 35–76.
- 63 M. V. Capparelli, D. M. Goodgame, P. B. Hayman, A. C. Shapski, *J. Chem. Soc., Chem. Commun.*, 1986, 776–777.
- 64 V. W. Day, W. G. Klemperer, D. J. Maltbie, *J. Am. Chem. Soc.*, 1987, **109**, 2991–3002.
- 65 C. Djordjevic, M. Lee, E. Sinn, *Inorg. Chem.*, 1989, **28**, 719–723.
- 66 I. Csoregh, P. Kierkegaard, J. Legendzicz, E. Huskowska, *Acta Chem. Scand.*, 1989, **43**, 636–640.
- 67 P. A. Durif, M. T. Averbuch-Pouchot, J. C. Guitel, *Acta Crystallogr., Sect. B: Struct. Sci.*, 1980, **36**, 680–682.
- 68 I. Cherny, E. Gazit, *Angew. Chem., Int. Ed.*, 2008, **47**, 4062–4069.
- 69 C. H. Girbitz, *Chem. Eur. J.*, 2001, **7**, 5153–5159.
- 70 V. Jayawarna, M. Ali, T. A. Jowitt, A. E. Miller, A. Saiani, J. E. Gough, R. V. Ulijn, *Adv. Mater.*, 2006, **18**, 611–614.
- 71 A. Mahler, M. Reches, M. Rechter, S. Cohen, E. Gazit, *Adv. Mater.*, 2006, **18**, 1365–1370.
- 72 Y. Wang, M. Lingenfelder, T. Classen, G. Costantini, K. Kern, *J. Am. Chem. Soc.*, 2007, **129**, 15742–15743.
- 73 X. Yan, Q. He, K. Wang, L. Duan, Y. Cui, J. Li, *Angew. Chem.*, 2007, **119**, 2483–2486.
- 74 X. Yan, Y. Cui, Q. He, K. Wang, J. Li, W. Mu, B. Wang, Z. Ouyang, *Chem.-Eur. J.*, 2008, **14**, 5974–5980.
- 75 X. Yan, P. Zhu, J. Fei, J. Li, *Adv. Mater.*, 2010, **22**, 1283–1287.
- 76 R. Nishiyabu, N. Hashimoto, T. Cho, K. Watanabe, T. Yasunaga, A. Endo, K. Kaneko, T. Niidome, M. Murata, C. Adachi, Y. Katayama, M. Hashizume, N. Kimizuka, *J. Am. Chem. Soc.*, 2009, **131**, 2151–2158.
- 77 I. Imaz, J. Hernando, D. Ruiz-Molina, D. MasPOCH, *Angew. Chem. Int. Ed.*, 2009, **48**, 2325–2329.
- 78 Z. Ma, Y. Qiu, H. Yang, Y. Huang, J. Liu, Y. Lu, C. Zhang, P. A. Hu, *ACS Appl. Mater. Interfaces*, 2015, **7**, 22036–22045.
- 79 K. S. Kosik, *Science*, 1992, **256**, 780–783.
- 80 G. Yamin, K. Ono, M. Inayathullah, D. B. Teplow, *Curr. Pharm. Des.*, 2008, **14**, 3231–3246.
- 81 H.-U. Bernard, *Infect. Genet. Evol.*, 2013, **18**, 357–361.
- 82 E.-M. Villiers, C. Fauquet, T. R. Broker, H.-U. Bernard, H. Hausen, *Virology*, 2004, **324**, 17–27.
- 83 N. D. Christensen, *Expert Opin. Emerging Drugs*, 2005, **10**, 5–19.
- 84 H. zurHausen, E. M. de Villiers, *Annu. Rev. Microbiol.*, 1994, **48**, 427–447.
- 85 E. P. Aggelopoulou, D. Skarlos, C. Papadimitriou, C. Kittas, C. Troungos, *Anticancer Res.*, 1999, **19**, 1391–1395.

- 86 T. Zhang, H.-W. Li, Y. Wu, Y. Wang, L. Wu, *J. Phys. Chem. C*, 2015, **119**, 8321–8328.
- 87 T. Zhang, H.-W. Li, Y. Wu, Y. Wang, L. Wu, *Chem. Eur. J.*, 2015, **21**, 9028–9033.
- 88 T. Zhang, D.-Y. Fu, Y. Wu, Y. Wang, L. Wu, *RSC Adv.*, 2016, **6**, 28612–28618.
- 89 T. Zhang, D.-Y. Fu, Y. Wu, Y. Wang, L. Wu, *Dalton Trans.* 2016, DOI: 10.1039/c6dt02186g.
- 90 A. G. Cherstvy, *Phys. Chem. Chem. Phys.*, 2011, **13**, 9942–9968.
- 91 H. Schiessel, *J. Phys. Condens. Matter*, 2003, **15**, 699–774.
- 92 S. Faham, R. E. Hileman, J. R. Fromm, R. J. Linhardt, D. C. Rees, *Science*, 1996, **271**, 1116–1120.
- 93 B. J. Zern, H. Chu, A. O. Osunkoya, J. Gao, Y. Wang, *Adv. Funct. Mater.*, 2011, **21**, 434–440.
- 94 P. Chairatana, E. M. Nolan, *J. Am. Chem. Soc.*, 2014, **136**, 13267–13276.
- 95 S. Bulut, T. S. Erkal, S. Toksoz, A. B. Tekinay, T. Tekinay, M. O. Guler, *Biomacromolecules*, 2011, **12**, 3007–3014.
- 96 R. H. Mo, J. L. Zaro, W.-C. Shen, *Mol. Pharm.*, 2012, **9**, 299–309.
- 97 J. Li, Z. Chen, M. Zhou, J. Jing, W. Li, Y. Wang, L. Wu, L. Wang, Y. Wang, M. Lee, *Angew. Chem. Int. Ed.*, 2016, **55**, 2592–2595.
- 98 I. Choi, I.-S. Park, J.-H. Ryu, M. Lee, *Chem. Commun.*, 2012, **48**, 8481–8483.
- 99 B. Hasenknopf, K. Micoine, E. Lacote, S. Thorimbert, M. Malacria, R. Thouvenot, *Eur. J. Inorg. Chem.*, 2008, **32**, 5001–5013.
- 100 Y.-Q. Lan, S.-L. Li, X.-L. Wang, K.-Z. Shao, D.-Y. Du, Z.-M. Su, E.-B. Wang, *Chem. Eur. J.*, 2008, **14**, 9999–10006.
- 101 H.-Y. An, E.-B. Wang, D.-R. Xiao, Y.-G. Li, Z.-M. Su, L. Xu, *Angew. Chem.*, 2006, **118**, 918–922.
- 102 V. Soghomonian, Q. Chen, R. C. Haushalter, J. Zubieta, C. J. O'Connor, *Science*, 1993, **259**, 1596–1599.
- 103 M. Sadakane, M. H. Dickman, M. T. Pope, *Inorg. Chem.*, 2001, **40**, 2715–2719.
- 104 C. Boglio, B. Hasenknopf, G. Lenoble, P. Rmy, P. Gouzerh, S. Thorimbert, E. Lacote, M. Malacria, R. Thouvenot, *Chem. Eur. J.*, 2008, **14**, 1532–1540.
- 105 G. Lenoble, B. Hasenknopf, R. Thouvenot, *J. Am. Chem. Soc.*, 2006, **128**, 5735–5744.
- 106 C. Boglio, K. Micoine, E. Derat, R. Thouvenot, B. Hasenknopf, S. Thorimbert, E. Lacote, M. Malacria, *J. Am. Chem. Soc.* 2008, **130**, 4553–4561.
- 107 K. Micoine, B. Hasenknopf, S. Thorimbert, E. Lacote, M. Malacria, *Angew. Chem.*, 2009, **121**, 3518–3520.
- 108 K. B. Grant, M. Kassai, *Curr. Org. Chem.*, 2006, **10**, 1035–1049.
- 109 T. N. Parac, N. M. Kostic, *J. Am. Chem. Soc.*, 1996, **118**, 5946–5951.
- 110 N. M. Milovic, L. M. Dutca, N. M. Kostic, *Chem.-Eur. J.*, 2003, **9**, 5097–5106.
- 111 E. Kopera, A. Krezel, A. M. Protas, A. Belczyk, A. Bonna, A. Wyslouch-Cieszynska, J. Poznanski, W. Bal, *Inorg. Chem.*, 2010, **49**, 6636–6645.
- 112 M. Kassai, K. B. Grant, *Inorg. Chem. Commun.*, 2008, **11**, 521–525.
- 113 T. Takarada, M. Yashiro, M. Komiyama, *Chem.-Eur. J.*, 2000, **6**, 3906–3913.
- 114 P. H. Ho, K. Stroobants, T. N. Parac-Vogt, *Inorg. Chem.*, 2011, **50**, 12025–12033.
- 115 S. Vanhaecht, G. Absillis, T. N. Parac-Vogt, *Dalton Trans.*, 2012, **41**, 10018–10034.
- 116 G. Absillis, T. N. Parac-Vogt, *Inorg. Chem.*, 2012, **51**, 9902–9910.
- 117 H. G. T. Ly, G. Absillis, S. R. Bajpe, J. A. Martens, T. N. Parac-Vogt, *Eur. J. Inorg. Chem.*, 2013, 4601–4611.
- 118 H. G. Ly, G. Absillis, T. N. Parac-Vogt, *Dalton Trans.* 2013, **42**, 10929–10938.
- 119 K. Stroobants, G. Absillis, E. Moelants, P. Proost, T. N. Parac-Vogt, *Chem. Eur. J.*, 2014, **20**, 3894–3897.
- 120 H. G. Ly, G. Absillis, R. Janssens, P. Proost, T. N. Parac-Vogt, *Angew. Chem. Int. Ed.* 2015, **54**, 7391–7394.
- 121 A. Sap, G. Absillis, T. N. Parac-Vogt, *Dalton Trans.* 2015, **44**, 1539–1548.
- 122 T. Quanten, P. Shestakova, D. Van Den Bulck, C. Kirschhock, T. N. Parac-Vogt, *Chem. - Eur. J.* 2016, **22**, 3775–3784.
- 123 Rauk, A. *Chem. Soc. Rev.*, 2009, **38**, 2698–2715.
- 124 R. Jakob-Roetne, H. Jacobsen, *Angew. Chem., Int. Ed.*, 2009, **48**, 3030–3059.
- 125 E. Gaggelli, H. Kozlowski, D. Valensin, G. Valensin, *Chem. Rev.*, 2006, **106**, 1995–2044.
- 126 I. W. Hamley, *Chem. Rev.*, 2012, **112**, 5147–5192.
- 127 L. E. Cassagnes, V. Herve, F. Nepveu, C. Hureau, P. Faller, F. Collin, *Angew. Chem., Int. Ed.*, 2013, **52**, 11110–11113.
- 128 J. T. Pedersen, C. Hureau, L. Hemmingsen, N. H. H. Heegaard, J. Ostergaard, M. Vasak, P. Faller, *Biochemistry*, 2012, **51**, 1697–1706.
- 129 M. Richman, S. Wilk, N. Skirtenko, A. Perelman, S. Rahimipour, *Chem. Eur. J.*, 2011, **17**, 11171–11177.
- 130 H. LeVine III, *Protein Sci.*, 1993, **2**, 404–410.
- 131 ME Davis, ZG Chen, DM Shin, *Nat. Rev. Drug Discov.*, 2008, **7**, 771–822.
- 132 W. Qi, L. Wu, *Polym. Int.*, 2009, **58**, 1217–1225.
- 133 Z. Zhang, L. Zhou, Y. Zhou, J. Liu, X. Xing, J. Zhong, G. Xu, Z. Kang, J. Liu, *Biomaterials*, 2015, **65**, 56–65.
- 134 K. Zhao, G.M. Zhao, D. Wu, Y. Soong, A.V. Birk, P.W. Schiller, H.H. Szeto, *J. Biol. Chem.*, 2004, **279**, 3468–34690.
- 135 X. Yan, J. Li, H. Mohwald, *Adv. Mater.*, 2012, **24**, 2663–2667.
- 136 X Yan, Y Su, J. Li, J. Früh, H. Mçhwald, *Angew. Chem. Int. Ed.* 2011, **50**, 11186–1119.
- 137 J. Ryu, S. Y. Lim, C. B. Park, *Adv. Mater.*, 2009, **21**, 1577–1581.
- 138 Z. Ma, Y. Qiu, H. Yang, Y. Huang, J. Liu, Y. Lu, C. Zhang, P. Hu, *ACS Appl. Mater. Interfaces*, 2015, **7**, 22036–22045.
- 139 H. Jin, D. A. Heller, M. Kalbacova, J.-H. Kim, J. Zhang, A. A. Boghossian, N. Maheshri, M. S. Strano, *Nat. Nanotechnol.*, 2010, **5**, 302–309.
- 140 H. Wei, E. Wang, *Anal. Chem.*, 2008, **80**, 2250–2254.
- 141 L. Gao, J. Zhuang, L. Nie, J. Zhang, Y. Zhang, N. Gu, T. Wang, J. Feng, D. Yang, S. Perrett, X. Yan, *Nat. Nanotechnol.*, 2007, **2**, 577–583.
- 142 F. Olucha, F. Martínez-García, C. Lopez-García, *J. Neurosci. Methods*, 1985, **13**, 131–138.
- 143 C. Mateo, J. M. Palomo, G. Fernandez-Lorente, J. M. Guisan, R. Fernandez-Lafuente, *Enzyme Microb. Technol.*, 2007, **40**, 1451–1463.
- 144 N. C. Veitch, *Phytochemistry*, 2004, **65**, 249–259.
- 145 J. Wang, D. Han, X. Wang, B. Qi, M. Zhao, *Biosens. Bioelectron.*, 2012, **36**, 18–21.
- 146 Y. Song, K. Qu, C. Zhao, J. Ren, X. Qu, *Adv. Mater.*, 2010, **22**, 2206–2210.
- 147 P. He, B. Xu, Wang, P. P, H. Liu, X. Wang, *Adv. Mater.* 2014, **26**, 4339–4344.



This review presents an overview of recent work focusing on the co-assembly of peptides and POMs, especially, their biological applications.